



Metabolic and functional distinction of the *Smicronyx* sp. galls on *Cuscuta campestris*

Lyuben I. Zagorchev¹ · Ivanela A. Albanova¹ · Anita G. Tosheva² · Junmin Li³ · Denitsa R. Teofanova¹

Received: 13 February 2018 / Accepted: 23 May 2018 / Published online: 28 May 2018
© Springer-Verlag GmbH Germany, part of Springer Nature 2018

Abstract

Main conclusion The weevil gall contains two distinct regions, differing in hydrolytic and antioxidant enzymes activity and profiles, which is also functionally distinct from the non-infected *Cuscuta* stems.

Weevils of the genus *Smicronyx* are gall-forming insects, widely distributed on parasitic flowering plants of the genus *Cuscuta*. Thus, they are considered epiparasites and potential method for biological control of their agriculturally harmful hosts. Although several reports on gall formation in *Cuscuta* spp. exist, the metabolic and functional changes, occurring in the gall, remained largely unknown. *Smicronyx* sp. galls, collected from a wild *Cuscuta campestris* population, were dissected into two distinct regions, inner and outer cortex, defined by the higher chlorophyll content of the inner cortex. Based on hydrolytic and antioxidant enzymes activity and isoenzymatic profiles as analyzed after electrophoretic separation, we suggested that the gall differs in its metabolic activity from the non-infected plant tissue. While the outer cortex serves as a region of nutrient storage and mobilization, the inner cortex is directly involved in larvae nutrition. The increase in metabolic activity resulted in significantly increased superoxide dismutase activity in the gall, while several other antioxidant enzymes diminished. The present research offers new insights into the functionally differing regions of *Smicronyx* galls and the metabolic changes, induced in *C. campestris* in result of the gall formation.

Keywords Antioxidant enzymes · Insect galls · Parasitic plants · Hydrolytic enzymes

Introduction

Cuscuta campestris Yunck. or field dodder is a stem holoparasitic flowering plant of the family Convolvulaceae, widely distributed in temperate and subtropical ecosystems (Benvenuti et al. 2005). It is native to North America, but currently introduced and considered invasive globally. Field dodder seeds are often distributed as contamination of seeds

of clovers (*Trifolium* spp.) and alfalfa (*Medicago sativa* L.) or soil (Parker 2012). In agriculture, it is one of the most important pests among members of the genus *Cuscuta*, causing significant yield losses, especially in alfalfa, sugar beet (*Beta vulgaris* L.), and other crop species. The devastating effect is caused by significant growth reduction of the host plants. Being non-photosynthetic parasitic plants, dodders attach to and penetrate the phloem of multiple hosts. They extract water, mineral nutrients, and organic compounds from the infected plants through haustoria (Haupt et al. 2001). The metabolic sink could account for up to 81% of the current photosynthates and more than twofold of the organic nitrogen, available before infection (Jeschke et al. 1994). By representing such a substantial sink, dodders significantly reduce biomass accumulation and seeds development of infested host plants. The control strategies include complete mechanical eradication of both the parasite and the infected hosts (Parker 2012) as herbicides often proved to be inefficient or equally damaging to crops (Tepe et al. 2017),

✉ Lyuben I. Zagorchev
lzagorchev@biofac.uni-sofia.bg

¹ Department of Biochemistry, Faculty of Biology, Sofia University “St. Kliment Ohridski”, 8 Dragan Tsankov Blvd., 1164 Sofia, Bulgaria

² Department of Botany, Faculty of Biology, Sofia University “St. Kliment Ohridski”, 8 Dragan Tsankov Blvd., 1164 Sofia, Bulgaria

³ Zhejiang Provincial Key Laboratory of Plant Evolutionary Ecology and Conservation, Taizhou University, Taizhou 318000, China

as well as crop rotation and introduction of *Cuscuta*-resistant cultivars (Tjiurutue et al. 2016).

Recently, the possibility for biological control of dodders has gained attention. Trials include fungal pathogens (Falahpour et al. 2016) and coleopteran parasites of the genus *Smicronyx* Schönherr, 1843 (Coleoptera, Curculionidae), or weevils (Zhekova et al. 2014). Several weevil species express specific preference to *Cuscuta* spp. as hosts and were found to cause substantial growth retardation, prevent flowering and seed formation, and eventually lead to death of infected dodders (Sandler 2010). *Smicronyx* spp. larvae induce the formation of characteristic spherical galls, left after reaching full maturity (Zhekova et al. 2014). Although numerous studies were performed to estimate the biological control value of different *Smicronyx* species, very little was done to follow the biochemical changes, occurring in the gall. Recently, it was found that the core of the *Smicronyx smreczynskii* galls on *C. campestris* contained significantly higher chlorophyll concentrations and leads to increase in the functional PSII reaction centers, thus causing actual photosynthesis to occur in a typically non-photosynthetic plant (Anikin et al. 2017). Such a dramatic change in functionality, most probably beneficial to the larvae, establishes the formed gall as a physiologically distinct plant structure, differing in metabolic activity to the other sections of the dodder. In other insect galls, however, multiple biochemical events were identified such as reactive oxygen species (ROS) production (de Oliveira et al. 2014) and gradients of metabolites in different gall sections (Carneiro and Isaias 2015). Such processes suggest the involvement of a variety of ROS—scavenging enzymes as well as hydrolytic enzymes, related to the mobilization of storage compounds, used in the larvae nutrition (de Oliveira et al. 2014). Accordingly, it is expected that such enzymes will differ in both activity and profiles in the gall compared to non-infected plant tissues.

Zymographic analysis, e.g., the detection of enzymatic activities after electrophoretic separation, allows simultaneous identification of different isoforms of particular enzymes. Currently, hundreds of enzymes are possible to be detected on polyacrylamide gels (Manchenko 2002). Such analytical techniques proved to be useful tools to follow the differential activity of numerous antioxidant, hydrolytic etc. isoenzymes in a spatial (in separate tissues) and temporal (during different stages of development) manner. Particularly, in *Cuscuta* spp., zymography was used to detect differential expression of peroxidase isoforms, involved in the formation of haustoria (Svubova et al. 2017). Zymographic analyses were also used to identify stress-related antioxidant enzymes (Zhang et al. 2013), detection of somatic embryogenesis associated proteases (Rakleova et al. 2010), wheat β -glucosidase in seedlings (Sue et al. 2000), and many more. By such, it is also suitable to identify specific isoenzymes, appearing or disappearing in *Cuscuta* galls. Using

zymographic techniques, the current study aims to follow the activity and possible new isoforms of antioxidant and hydrolytic enzymes in the *Smicronyx* galls in comparison to non-infected *Cuscuta* stem.

Materials and methods

Cuscuta campestris/*Smicronyx* galls

Cuscuta campestris Yunck. was collected from a wild population in Sofia region, Sofia, Cherni Vrah Blvd, 42°39'03.7"N 23°18'56.7"E and kept fresh until further analyses. A voucher herbarium material was deposited in Sofia University Herbarium (SO) under the number SO 107783. The species was determined according to morphological characteristics by Dr. Anita Tosheva. Collection time was in mid-June, 2017 when most of the galls have living larvae inside. Galls were identified as *Smicronyx* spp. galls by the characteristic shape and the morphology of the larvae. The exact species was not identified as no adult specimens were available. Plant material for analyses was cut into inner gall cortex, outer gall cortex, adjacent stem section (5 mm from both ends of the gall), and non-infected stem. Chlorophyll concentration was measured spectrophotometrically in grounded to powder in liquid nitrogen material, dissolved in 80% (v/v) acetone. After centrifugation at 10,000 g for 15 min at 4 °C, the absorbance specter of the supernatants was measured on NanoDrop 2000 spectrophotometer. Pigment concentration (in $\mu\text{g ml}^{-1}$) was calculated according to the following equations (Sumanta et al. 2014):

$$\text{Chlorophyll a} = 12.25 \times A_{663.2} - 0.279 \times A_{646.8}$$

$$\text{Chlorophyll b} = 21.5 \times A_{646.8} - 5.1 \times A_{663.2}$$

Chlorophylls were measured separately in five individual galls.

Protein isolation and polyacrylamide gel electrophoresis

Water-soluble proteins were extracted with PBS, pH 7.2, supplemented with protease inhibitor cocktail (Sigma) from approximately 100 mg of liquid nitrogen grounded tissue. The supernatant after centrifugation for 15 min at 15,000 g at 4 °C, containing the soluble proteins, was used for subsequent analyses. Protein concentration was measured with Pierce BCA protein assay kit according to instruction manual. A total of 15 μg protein was loaded onto wells of Cleaver Scientific Omnipage Mini electrophoretic system. Separation was on 12.5% T SDS PAGE according to the protocol of Laemmli (1970), followed by renaturation in 2.5% (v/v) Triton[®] X-100 for 20 min on a

shaker. Zymographic analyses were performed according to Manchenko (2002), unless otherwise stated. The following enzymes were studied:

Antioxidant enzymes

Peroxidases (POD; EC 1.11.1.7) were visualized with 2.5 mM H₂O₂ and 9 mM guaiacol in PBS, pH 7.2. Gels were immersed in the staining solution on a shaker until dark orange bands appeared and immediately photographed. For L-ascorbate peroxidases (APX; EC 1.11.1.11), gels were equilibrated in 50 mM sodium phosphate buffer pH 7.0 with 2 mM ascorbate, then incubated for 20 min in the same buffer with 4 mM ascorbate and 2 mM H₂O₂, washed for 1 min, and stained in 28 mM TEMED, 2.45 mM NBT in sodium phosphate buffer pH 7.8 until achromatic bands appeared on dark blue background. Superoxide dismutase (SOD; EC 1.15.1.1) was visualized by incubation with 1 mg ml⁻¹ NBT for 10 min, followed by UV illumination in a solution of 0.01 mg ml⁻¹ riboflavin, 28 mM TEMED in sodium phosphate buffer pH 7.8 until achromatic bands appeared on dark blue background. For glutathione reductase activity (GR; EC 1.6.4.2), electrophoreses were performed under non-denaturing conditions (SDS omitted in gels, sample buffer and running buffer). After electrophoresis, the gels were overlaid by a replica gel, containing 1.5 mg ml⁻¹ glutathione disulphide (GSSG), 0.5 mg ml⁻¹ NADPH and 1% (w/v) agarose in 0.15 M TRIS.HCl pH 8.0 and incubated in the dark for 30 min. Subsequently, the replica gel was photographed on UV transilluminator and GR isozymes appeared as dark bands on fluorescent background. Catalases (CAT; EC 1.11.1.6) were visualized by incubation of the gels (pre-cast with 0.2% (w/v) soluble starch) in 3% (v/v) H₂O₂ and 90 mM KI until achromatic bands appeared on dark blue background.

Hydrolytic enzymes

For proteases (PROT; EC 3.4.21–24), proteins were separated in 12.5% T SDS PAGE, containing 0.2% (w/v) gelatin in the running gel. After renaturation, the gels were incubated at 37 °C for 12 h in 200 mM NaCl, 5 mM CaCl₂ in 50 mM TRIS.HCl pH 8.8, followed by staining in 0.1% (w/v) Coomassie Brilliant Blue R-250 in 40% (v/v) methanol, 10% (v/v) acetic acid until achromatic bands appeared on dark blue background. For α-amylase (AMY; EC 3.2.1.1) activity, proteins were separated in gels, containing 0.2% (w/v) soluble starch, and incubated for 12 h in 20 mM CaCl₂ in 50 mM sodium acetate buffer pH 5.6 at 37 °C, followed by staining in 3% (v/v) H₂O₂ and 90 mM KI until achromatic bands appeared on dark blue background.

Software processing of gel images and statistical analysis

All gels were run in triplicates with proteins, isolated from individual galls, and photographed on a gel imaging system (Syngene). Molecular weights were determined on Gel Analyzer 2010a, using molecular weight standards PageRuler™ 10–250 kDa Prestained Protein Ladder (Thermo Scientific). All zymograms, resulting in achromatic bands on colored background, were processed with the inverse function of Adobe Photoshop CC 2015 to acquire dark bands on light background for better visualization. Activity of individual isoenzymes was calculated by the peaks' areas on ImageJ 1.51j. The overall relative activity was measured by the sum of all peaks in the particular sample with the relative activity of non-infected stem equalized to 1. Student's *t* test was performed to indicate statistical significance at *P* < 0.05.

Results

Smicronyx galls

Smicronyx sp. galls were abundant in the studied *C. campestris* population and non-infected plants were not found. Galls were formed at either the basis of the inflorescences or throughout the stem. No galls were found on the *Cuscuta* host species, which was predominantly *Trifolium* sp. The average size of galls were 1.5–2.5 cm long and 0.5–0.8 cm wide, usually fusiform according to morphotypes, summarized by Isaias et al. (2013) or with irregular shape (Fig. 1a) with a larva inside (Fig. 1b). In approximately 30% of the collected galls, no larvae were found and 5% were punctured and also empty. It was assumed that in the latter case, the larvae already completed the metamorphosis to adult weevils. For the purpose of the further experimental work, all empty galls were excluded. The cross section of the galls revealed two distinct regions—a greenish inner cortex around the larval chamber and a pale-yellow outer cortex (Fig. 1c). Spectrophotometric determination of chlorophyll concentration showed significant increase of both chlorophyll A and chlorophyll B in the gall, compared to stem (Fig. 2). Chlorophyll A increased almost twofold in the outer cortex and over threefold in the inner cortex of the gall. Chlorophyll B was not detected in the non-infected stems and also in the highest concentration in the inner cortex.

Hydrolytic enzymes

Protease activity zymograms revealed four distinct protease isoforms named PROT1-4 with molecular weights ranging from 49 to 98 kDa (Fig. 3a, b). Two of the isoforms were not detected in non-infected stems and in the stem section

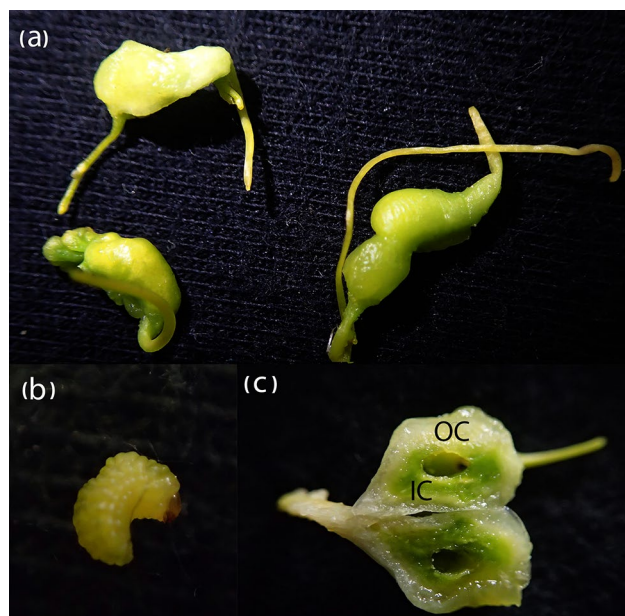


Fig. 1 *Smicronyx* sp. galls (a) and *Smicronyx* sp. larva (b), found on *Cuscuta campestris* stem. The transverse cut (c) reveals two distinct layers around the larva, a greenish inner cortex (IC) and a pale white outer cortex (OC)

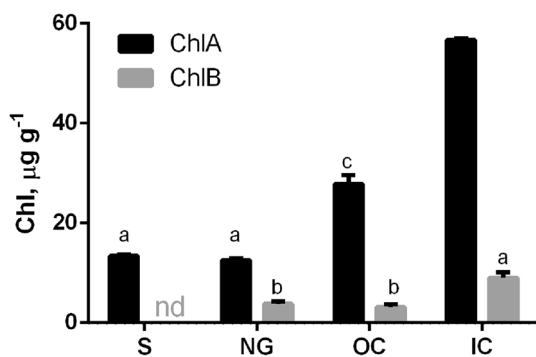


Fig. 2 Concentration of chlorophyll A and chlorophyll B in non-infected *Cuscuta campestris* stems (S), *Cuscuta* stem up to 5 mm of the *Smicronyx* gall, e.g., near gall (NG), outer cortex (OC) and inner cortex (IC) of the gall. nd not detected. Different letters indicate significance at $P < 0.05$, Student's t test

in proximity to the gall. All of the isoforms increased in relative activity in the inner and outer cortex of the gall (Fig. 3c). The isoform PROT3 with molecular weight of 56 kDa showed the highest relative activity. Overall, the combined activity relative to the non-infected stems based on the combined peak area of all isoforms increased gradually with almost tenfold increase in the outer cortex, but slightly lower in the inner cortex of the gall (Fig. 3d).

Six α -amylase isoforms were detected, of which four, AMYL1-4 with molecular weight ranging from 50 to

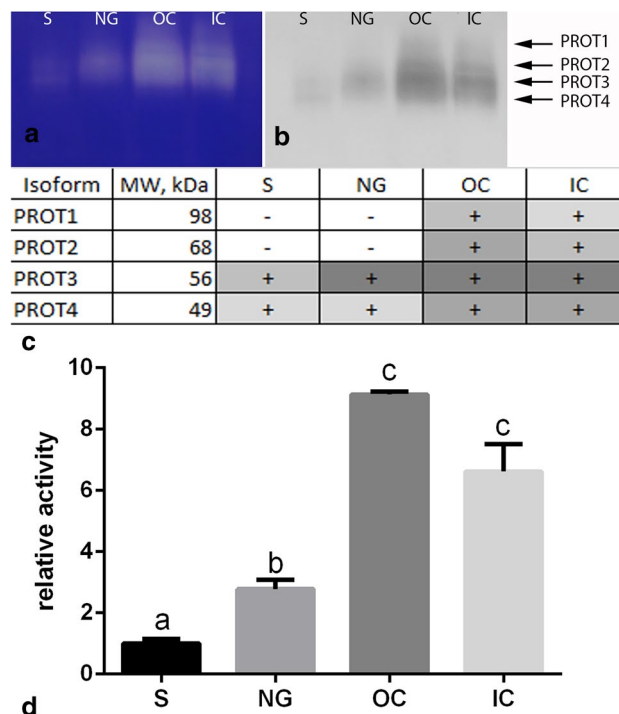


Fig. 3 Protease (PROT) isoforms and relative activity in non-infected *Cuscuta campestris* stems (S), near gall (NG), outer cortex (OC) and inner cortex (IC) of the gall. a Original zymogram; b software enhanced zymogram; c molecular weight in kDa and apparent activity of detected PROT isoforms. Activity increase from white (– not presented) to dark grey (+ presented); d combined activity of all isoforms, relative to the activity in stems (S), which is assumed as 1. Error bars show standard deviation, $n=3$. Different letters indicate significance at $P < 0.05$, Student's t test

120 kDa were presented in all studied samples and with similar starch hydrolytic activity (Fig. 4a–c). Two α -amylase isoforms with lower molecular weight, AMYL5 and six were presented only in the inner and outer cortex of the galls (Fig. 4a, b). AMYL5 (M_w 30 kDa) was also presented in the non-infected stems in trace amount, but with distinctly higher activity in the outer cortex of the gall (Fig. 4c). The combined relative activity showed similar pattern to the protease activity, although the increase in both regions of the gall was not so pronounced (Fig. 4d).

Antioxidant enzymes

The five studied antioxidant enzymes could be divided into two groups, depending on whether the activity increased or decreased in the galls. The enzymes with decreased activity in the gall were ascorbate peroxidase, catalase and glutathione reductase. Single ascorbate peroxidase (APX1, M_w 24 kDa, Fig. 5a, b) and catalase (CAT1, M_w 55 kDa, Fig. 6a, b) isoforms were detected and showed gradually decreasing activity (Figs. 5c, d, 6c, d) from non-infected

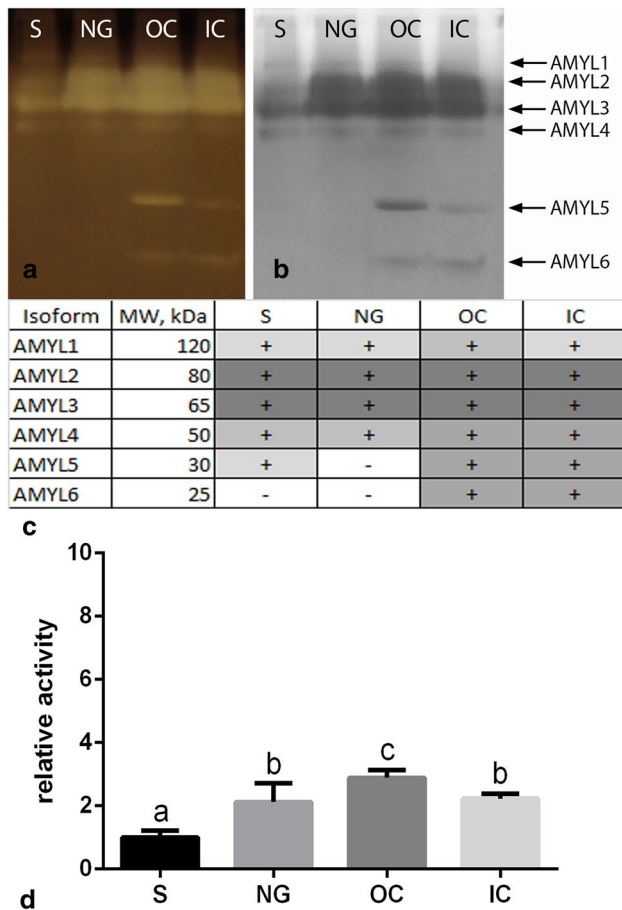


Fig. 4 α-Amylase (AMYL) isoforms and relative activity in non-infected *Cuscuta campestris* stems (S), near gall (NG), outer cortex (OC) and inner cortex (IC) of the gall. **a** Original zymogram; **b** software enhanced zymogram; **c** molecular weight in kDa and apparent activity of detected AMYL isoforms. Activity increase from white (– not presented) to dark grey (+ presented); **d** combined activity of all isoforms, relative to the activity in stems (S), which is assumed as 1. Error bars show standard deviation, $n=3$. Different letters indicate significance at $P<0.05$, Student’s t test

stems toward the inner cortex of the gall. A similar pattern was observed for glutathione reductase (Fig. 7). The less active isoform GR2 was also not detected in the inner and outer cortex of the gall (Fig. 7c). The relative activity decreased substantially in the gall for all three enzymes to 0.1 in the inner cortex (Figs. 5d, 6d, 7d).

A total of five guaiacol peroxidase isoforms were detected with a 150 kDa POD1 detected only in stems and decreasing in the stem section in proximity to the gall (Fig. 8a, b). The 124 kDa POD2 and 25 kDa POD5 showed the highest activity in the outer cortex of the gall (Fig. 8c). The relative combined activity was highest in the outer cortex, but decreased in the inner cortex of the gall (Fig. 8d). All four superoxide dismutase isoforms increased in activity from non-infected stem to the inner cortex of the gall (Fig. 9a–c). The combined activity of

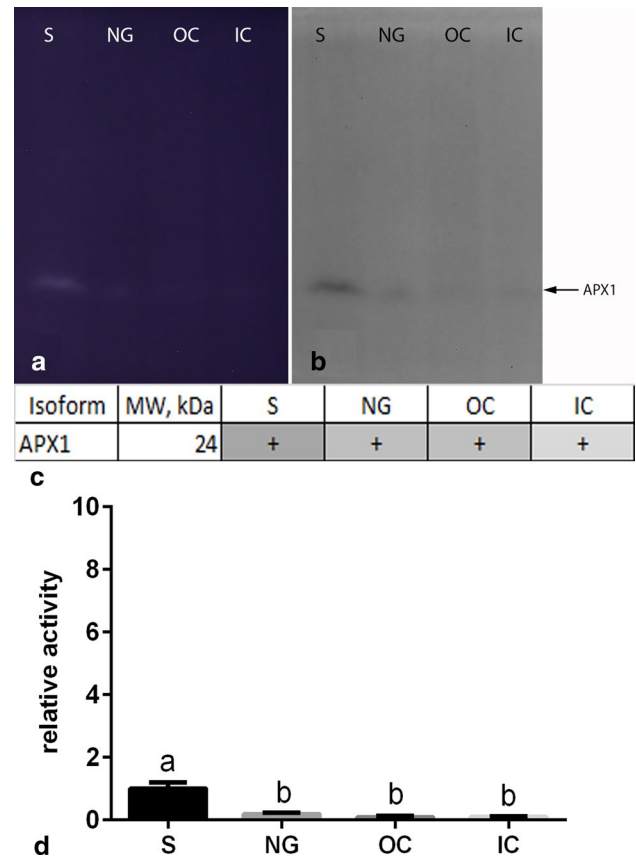


Fig. 5 Ascorbate peroxidase (APX) isoforms and relative activity in non-infected *Cuscuta campestris* stems (S), near gall (NG), outer cortex (OC) and inner cortex (IC) of the gall. **a** Original zymogram; **b** software enhanced zymogram; **c** molecular weight in kDa and apparent activity of detected APX isoforms. Activity increase from white (– not presented) to dark grey (+ presented); **d** combined activity of all isoforms, relative to the activity in stems (S), which is assumed as 1. Error bars show standard deviation, $n=3$. Different letters indicate significance at $P<0.05$, Student’s t test

SOD raised gradually with almost tenfold increase in the inner layer (Fig. 9d).

Discussion

The most obvious phenotypic distinction between the gall tissue and the non-infected *C. campestris* stem is the accumulation of chlorophyll, especially in the greenish inner cortex of the gall (Fig. 1c). The cross section of the galls was very similar to the previous reports (Zhekova et al. 2014; Anikin et al. 2017), showing larval chamber, surrounded by the chlorophyll-rich inner cortex and the paler outer cortex (Fig. 1c). The increased chlorophyll concentration (Fig. 2) in the inner cortex confirmed the possibility that *Smicronyx* galls on *Cuscuta* are photosynthetically active (Anikin et al. 2017), which is a substantial difference in functionality of

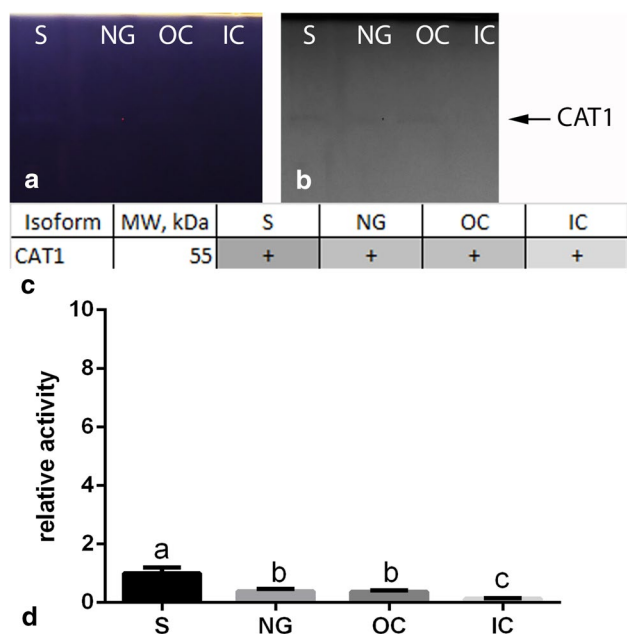


Fig. 6 Catalase (CAT) isoforms and relative activity in non-infected *Cuscuta campestris* stems (S), near gall (NG), outer cortex (OC) and inner cortex (IC) of the gall. **a** Original zymogram; **b** software enhanced zymogram; **c** molecular weight in kDa and apparent activity of detected CAT isoforms. Activity increase from white (– not presented) to dark grey (+ presented); **d** combined activity of all isoforms, relative to the activity in stems (S), which is assumed as 1. Error bars show standard deviation, $n=3$. Different letters indicate significance at $P<0.05$, Student's t test

the gall, compared to *Cuscuta* tissue. Although there are species-specific differences, most of the *Cuscuta* spp. are considered non-photosynthetic in result of their adaptation to parasitic lifestyle. Accordingly, chlorophyll is not presented at all in some species, or, including *C. campestris*, is in several fold lower concentration than in photosynthetic plants (Van der Kooij et al. 2000). These results suggested that under specific conditions, *C. campestris* has a conserved ability to synthesize photosynthetic pigments and to perform photosynthesis. One such condition was reported relatively long time ago (Zimmermann 1962) when it was shown that under in vitro conditions (absence of host) and carbohydrate deficiency, *C. pentagona* may turn to autotrophic development. The major changes, associated with gall formation in *C. campestris*, lead to similar changes in functionality.

Gall formation is accompanied by reprogramming of plant development and formation of functionally diverse plant tissues, adapted to serve the insect larvae needs (Pawłowski et al. 2017). Increased photosynthetic rates were associated with insect-caused galls as a mechanism to compensate the resource sink toward the larvae (Dorchin et al. 2006). As the larval nutrition leads to substantial carbohydrate redistribution and loss, the plant tissue responds by enhanced photosynthesis to meet the increased needs for

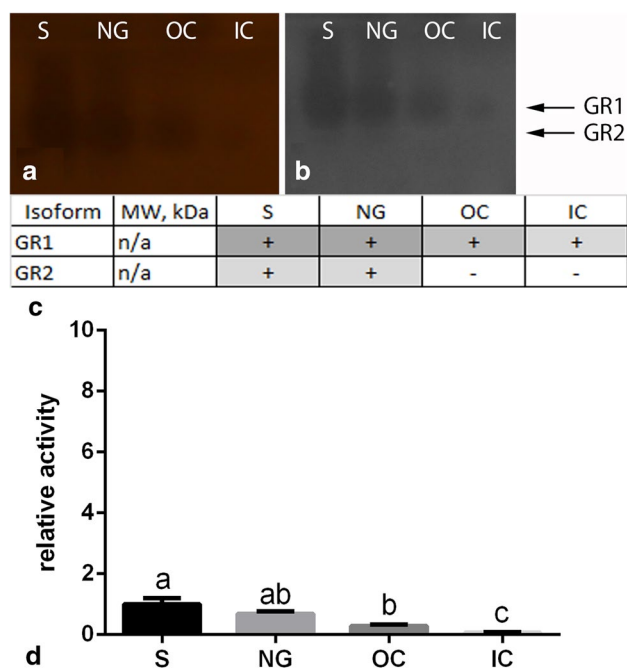


Fig. 7 Glutathione reductase (GR) isoforms and relative activity in non-infected *Cuscuta campestris* stems (S), near gall (NG), outer cortex (OC) and inner cortex (IC) of the gall. **a** Original zymogram; **b** software enhanced zymogram; **c** molecular weight in kDa and apparent activity of detected GR isoforms. Activity increase from white (– not presented) to dark grey (+ presented); **d** combined activity of all isoforms, relative to the activity in stems (S), which is assumed as 1. Error bars show standard deviation, $n=3$. Different letters indicate significance at $P<0.05$, Student's t test

photosynthates. A similar effect may be presented in *C. campestris* galls, where the carbohydrate sink toward the *Smicronyx* larvae leads to adaptive increase in chlorophyll concentration (Fig. 2) and increased photosynthetic rates (Anikin et al. 2017) as a response to carbohydrate deficiency. The present case, however, seems not be a universal case in insect galls. In many galls, the outer cortex is the chlorophyll rich, while photosynthetic rates were shown to be generally lower than in non-infected plant tissues (de Oliveira et al. 2014).

The activity of hydrolytic enzymes further supported the functional distinction between the inner and the outer cortex, as well as compared to the non-infected stems. Both proteases (Fig. 3) and α -amylases (Fig. 4) showed enhanced activity and several isoforms were detected only in galls, which is in correspondence with the previous finding that insect-induced plant galls are metabolically active, starch, and protein-rich structures (Giron et al. 2016). Increase of α -amylases activity in plant galls was previously reported (Dsouza and Ravishankar 2014) and is associated with larval nutrition. Similarly, increased protease activity suggests enhanced proteolysis, also related to accumulation of free amino acids and better larval nutrition (Giron et al. 2016).

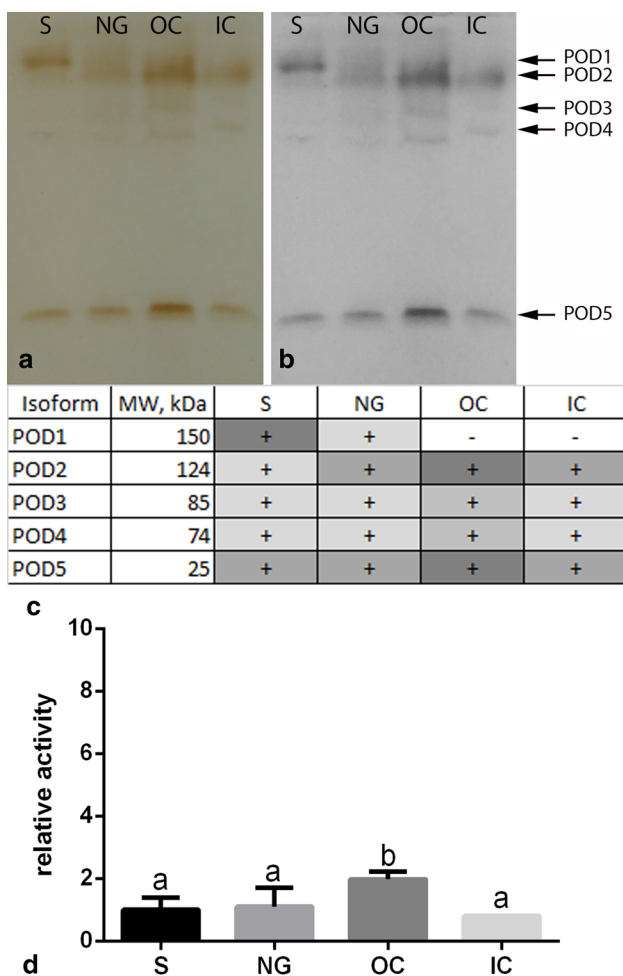


Fig. 8 Guaiacol peroxidase (POD) isoforms and relative activity in non-infected *Cuscuta campestris* stems (S), near gall (NG), outer cortex (OC) and inner cortex (IC) of the gall. **a** Original zymogram; **b** software enhanced zymogram; **c** molecular weight in kDa and apparent activity of detected POD isoforms. Activity increase from white (– not presented) to dark grey (+ presented); **d** combined activity of all isoforms, relative to the activity in stems (S), which is assumed as 1. Error bars show standard deviation, $n=3$. Different letters indicate significance at $P < 0.05$, Student’s t test

Notably, the activity of particular isoforms and overall activity was higher in the outer cortex. In functional aspect, these results support the previous findings of metabolic gradients in the gall tissue (de Oliveira et al. 2014). While the inner cortex is mainly involved in larval nutrition and provides amino acids and sugars, the outer cortex may serve as storage region for proteins and starch. Thus, the activity of both proteases and α -amylases supports the nutritional sink toward the larval chamber.

The increased metabolic and the suggested photosynthetic activity lead to significant increase in SOD activity, especially in the inner cortex of the gall (Fig. 9). This is essential for the scavenging of superoxide radicals, generated during photosynthesis even in optimal conditions

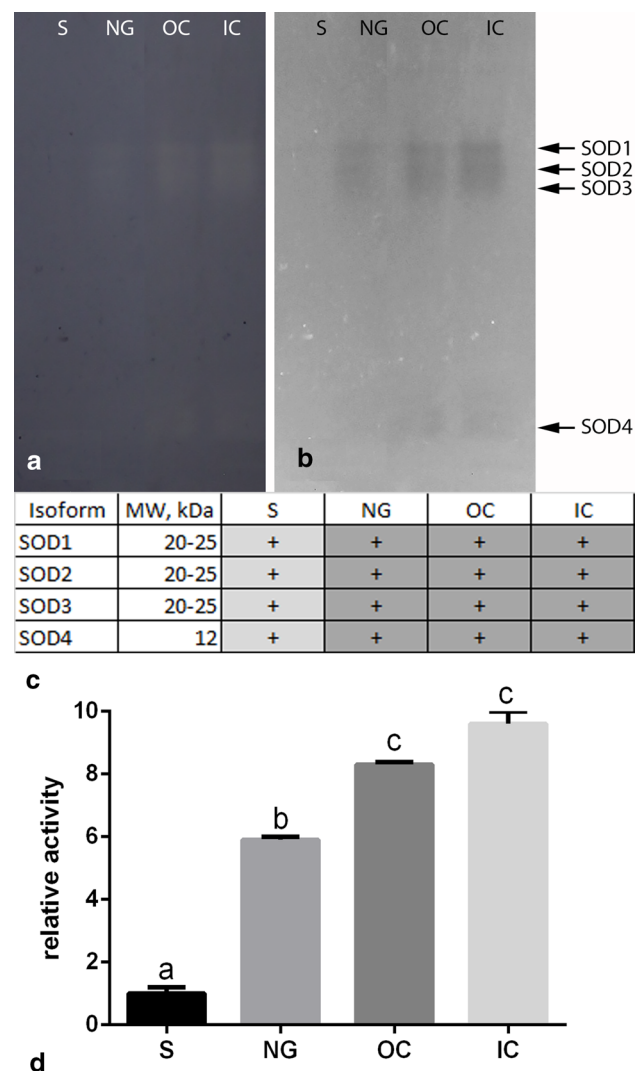


Fig. 9 Superoxide dismutase (SOD) isoforms and relative activity in non-infected *Cuscuta campestris* stems (S), near gall (NG), outer cortex (OC) and inner cortex (IC) of the gall. **a** Original zymogram; **b** software enhanced zymogram; **c** molecular weight in kDa and apparent activity of detected SOD isoforms. Activity increase from white (– not presented) to dark grey (+ presented); **d** combined activity of all isoforms, relative to the activity in stems (S), which is assumed as 1. Error bars show standard deviation, $n=3$. Different letters indicate significance at $P < 0.05$, Student’s t test

and the maintenance of the redox homeostasis (Foyer and Shigeoka 2011). The increase in SOD activity, however, was not accompanied by simultaneous increase in the connected CAT (Fig. 6) and two enzymes of the ascorbate glutathione cycle—APX (Fig. 5) and GR (Fig. 7). All of them are needed in the subsequent scavenging of H_2O_2 , produced in the superoxide dismutation and support the protection and repair of the photosynthetic systems (Foyer and Shigeoka 2011; Sae-Tang et al. 2016). Increased activities of these enzymes were expected because of the presumable oxidative burst

in the inner cortex of mature galls (de Oliveira et al. 2014; Isaias et al. 2015). Increased POD and CAT activities were observed in *Alstonia scholaris* R. Br. insect-induced galls (Biswas et al. 2014). Of these, only POD activity was higher in the outer cortex in *C. campestris* (Fig. 8), but diminished in the inner cortex, where the oxidative stress, caused by the larvae was supposed to be highest (de Oliveira et al. 2014). As it was shown that *Cuscuta* spp. could actively respond to stress factors (Cd ions) by increasing CAT, POD, and GR activities (Srivastava et al. 2004), we could suggest that the *Smicronyx*-induced oxidative stress is either not substantial or the larvae itself inhibited the antioxidant response. The significant increase in SOD activity should be attributed mainly to the altered metabolic activity in the gall rather than to stress response to the larvae itself.

In conclusion, we suggest that the formation of *Smicronyx* galls on *C. campestris* leads to the development of functionally distinct galls with metabolically well-defined inner and outer cortex. The inner cortex is chlorophyll rich and photosynthetically active (Anikin et al. 2017). It serves as direct nutritional source for the larvae, while the outer cortex is protective and storage region, where also the hydrolysis of starch and proteins mainly occurs. The major antioxidant response is related to the increased metabolic activity rather than oxidative stress, caused by the *Smicronyx* larvae.

Author contribution statement LIZ, JL and DRT designed the experiments and analyzed the data, AGT collected the plant samples and conducted species identification, IAA and DRT conducted the research, LIZ and JL wrote the article.

Acknowledgements The present study was financially supported by the National Science Fund of the Bulgarian Ministry of Education and Science, Grant DNTS China 01/5 and the Inter-governmental S&T Cooperation Proposal between Bulgaria and China (No. 15-2).

References

- Anikin V, Nikelshparg M, Nikelshparg E, Konyukhov I (2017) Photosynthetic activity of the dodder *Cuscuta campestris* (Convolvulaceae) in case of plant inhabitation by the gallformed weevil *Smicronyx smreczynskii* (Coleoptera, Curculionidae). *Izvestiya Saratov Univ New Ser Chem Biol Ecol* 17(1):42–47
- Benvenuti S, Dinelli G, Bonetti A, Catizone P (2005) Germination ecology, emergence and host detection in *Cuscuta campestris*. *Weed Res* 45(4):270–278
- Biswas SM, Chakraborty N, Pal B (2014) Foliar gall and antioxidant enzyme responses in *Alstonia scholaris*, R. Br. after psyllid herbivory—an experimental and statistical analysis. *Glob J Bot Sci* 2:12–20
- Carneiro RG, Isaias RM (2015) Gradients of metabolite accumulation and redifferentiation of nutritive cells associated with vascular tissues in galls induced by sucking insects. *Ann Bot Plants*. <https://doi.org/10.1093/aobpla/plv086>
- de Oliveira DC, Moreira ASFP, dos Santos Isaias RM (2014) Functional gradients in insect gall tissues: studies on Neotropical host plants. In: Fernandes JW, Santos JK (eds) *Neotropical insect galls*. Springer, Dordrecht, pp 35–49
- Dorchin N, Cramer MD, Hoffmann JH (2006) Photosynthesis and sink activity of wasp-induced galls in *Acacia pycnantha*. *Ecology* 87(7):1781–1791
- Dsouza M, Ravishankar B (2014) Nutritional sink formation in galls of *Ficus glomerata* Roxb. (Moraceae) by the insect *Pauropsylla depressa* (Psyllidae, Hemiptera). *Trop Ecol* 55(1):129–136
- Fallahpour F, Koocheki A, Mahallati MN, Rastegar MF, Ghorbani R (2016) Biological control of dodder (*Cuscuta campestris* L.) by fungi pathogens. *Büm/shinās-i kishāvarzī* 2(3):408–416
- Foyer CH, Shigeoka S (2011) Understanding oxidative stress and antioxidant functions to enhance photosynthesis. *Plant Physiol* 155(1):93–100
- Giron D, Huguet E, Stone GN, Body M (2016) Insect-induced effects on plants and possible effectors used by galling and leaf-mining insects to manipulate their host-plant. *J Insect Physiol* 84:70–89
- Haupt S, Oparka KJ, Sauer N, Neumann S (2001) Macromolecular trafficking between *Nicotiana tabacum* and the holoparasite *Cuscuta reflexa*. *J Exp Bot* 52(354):173–177
- Isaias RMS, Carneiro RGS, Oliveira DC, Santos JC (2013) Illustrated and annotated checklist of Brazilian gall morphotypes. *Neotrop Entomol* 42(3):230–239
- Isaias RMS, Oliveira DC, Moreira ASFP, Soares GLG, Carneiro RGS (2015) The imbalance of redox homeostasis in arthropod-induced plant galls: mechanisms of stress generation and dissipation. *Biochim et Biophys Acta (BBA) Gen Subj* 1850(8):1509–1517
- Jeschke WD, R ath N, B aumel P, Czygan F-C, Proksch P (1994) Modelling the flow and partitioning of carbon and nitrogen in the holoparasite *Cuscuta reflexa* Roxb. and its host *Lupinus albus* L. I. Methods for estimating net flows. *J Exp Bot* 45(6):791–800
- Laemmli UK (1970) Cleavage of structural proteins during the assembly of the head of bacteriophage T4. *Nature* 227(5259):680–685
- Manchenko GP (2002) *Handbook of detection of enzymes on electrophoretic gels*. CRC Press, Boca Raton
- Parker C (2012) Parasitic weeds: a world challenge. *Weed Sci* 60(2):269–276
- Pawłowski TA, Staszak AM, Karolewski P, Giertych MJ (2017) Plant development reprogramming by cynipid gall wasp: proteomic analysis. *Acta Physiol Plant* 39(5):114
- Rakleova G, Keightley A, Panchev I, Tsacheva I, Tchordadjieva M (2010) Cysteine proteinases and somatic embryogenesis in suspension cultures of orchardgrass (*Dactylis glomerata* L.). *Gen Appl Plant Physiol* 36(1–2):100–109
- Sae-Tang P, Hihara Y, Yumoto I, Orikasa Y, Okuyama H, Nishiyama Y (2016) Overexpressed superoxide dismutase and catalase act synergistically to protect the repair of PSII during photoinhibition in *Synechococcus elongatus* PCC 7942. *Plant Cell Physiol* 57(9):1899–1907
- Sandler HA (2010) Managing *Cuscuta gronovii* (swamp dodder) in cranberry requires an integrated approach. *Sustainability* 2(2):660–683
- Srivastava S, Tripathi RD, Dwivedi UN (2004) Synthesis of phytochelatin and modulation of antioxidants in response to cadmium stress in *Cuscuta reflexa*—an angiospermic parasite. *J Plant Physiol* 161(6):665–674
- Sue M, Ishihara A, Iwamura H (2000) Purification and characterization of a hydroxamic acid glucoside β -glucosidase from wheat (*Triticum aestivum* L.) seedlings. *Planta* 210(3):432–438
- Sumanta N, Haque CI, Nishika J, Suprakash R (2014) Spectrophotometric analysis of chlorophylls and carotenoids from commonly grown fern species by using various extracting solvents. *Res J Chem Sci* 2231:606X

- Svubova R, Lukacova Z, Kastier P, Blehova A (2017) New aspects of dodder–tobacco interactions during haustorium development. *Acta Physiol Plant* 39(3):66
- Tepe I, Celebi SZ, Kaya I, Ozkan RY (2017) Control of smoothseed alfalfa dodder (*Cuscuta approximata*) in alfalfa (*Medicago sativa*). *Int J Agric Biol* 19(1):199–203
- Tjiurutue MC, Sandler HA, Kersch-Becker MF, Theis N, Adler LA (2016) Cranberry resistance to dodder parasitism: induced chemical defenses and behavior of a parasitic plant. *J Chem Ecol* 42(2):95–106
- Van der Kooij T, Krause K, Dörr I, Krupinska K (2000) Molecular, functional and ultrastructural characterisation of plastids from six species of the parasitic flowering plant genus *Cuscuta*. *Planta* 210(5):701–707
- Zhang M, Fang Y, Ji Y, Jiang Z, Wang L (2013) Effects of salt stress on ion content, antioxidant enzymes and protein profile in different tissues of *Broussonetia papyrifera*. *S Afr J Bot* 85:1–9
- Zhekova E, Petkova D, Ivanova I (2014) *Smicronyx smreczynskii* F. Solari, 1952 (Insecta: Curculionidae): possibilities for biological control of two *Cuscuta* species (Cuscutaceae) in district of Ruse. *Acta Zool Bulg* 66(3):431–432
- Zimmermann C (1962) Autotrophic development of dodder (*Cuscuta pentagona* Englm.) in vitro. *Crop Sci* 2(5):449–450